

# $l_2$ - $l_\infty$ Proportional-Integral Observer Design for Systems with Mixed Time-Delays under Round-Robin Protocol

Di Zhao, Zidong Wang, Guoliang Wei\* and Fuad E. Alsaadi

## Abstract

In this paper, the design problem of  $l_2$ - $l_\infty$  proportional-integral observer (PIO) is investigated for a class of discrete-time systems with mixed time-delays. The mixed time-delays comprise both the discrete time-varying delays and infinitely distributed delays. The Round-Robin protocol (RRP) is employed to schedule the data transmissions from the sensors to the observer so as to mitigate the communication burden and prevent the data collisions. A novel PIO is developed whose observer gain is dependent on the data transmission order as a reflection of the effects induced by the RRP scheduling. By resorting to the token-dependent Lyapunov functional and the matrix inequality technique, the desired PIO is designed with exponentially stable error dynamics of the state estimation and guaranteed  $l_2$ - $l_\infty$  disturbance attenuation/resistance capacity. Finally, a simulation example is exploited to verify the validity of the proposed observer design method.

## Index Terms

Proportional-integral observer, Round-Robin protocol, mixed time-delays,  $l_2$ - $l_\infty$  performance.

## I. INTRODUCTION

FOR SEVERAL decades, the  $l_2$ - $l_\infty$  state estimation method has attracted persistent research attention since its inception in [8], [36] because of its great potential in assuring the disturbance rejection property of complex dynamic systems [38]. So far, the  $l_2$ - $l_\infty$  estimation/control problems have found wide applications in various areas such as aerospace, maneuvering target tracking, industrial process control, and so on [37]. Generally speaking, the  $l_2$ - $l_\infty$  state estimation problem aims to develop a state estimator with which the  $l_2$ - $l_\infty$  (energy-to-peak) gain from the disturbance input to the estimation error is less than a prespecified level. From a technical perspective, there are essentially two methods for designing the  $l_2$ - $l_\infty$  state estimators, namely, the Riccati difference/differential equation method and the linear matrix

The Deanship of Scientific Research (DSR) at King Abdulaziz University, Jeddah, Saudi Arabia funded this project under grant no. (FP-21-42). This work was also supported by the National Natural Science Foundation of China under Grants 61933007, 61873148 and 61873169, and the Alexander von Humboldt Foundation of Germany.

D. Zhao is with the College of Science, the Biomedical Engineering Postdoctoral Mobile Station, University of Shanghai for Science and Technology, Shanghai 200093, China. (Email: zhaodi0907520@163.com)

Z. Wang is with the Department of Computer Science, Brunel University London, Uxbridge, Middlesex, UB8 3PH, United Kingdom. (Email: Zidong.Wang@brunel.ac.uk)

G. Wei is with the College of Science, University of Shanghai for Science and Technology, Shanghai 200093, China. (Email: guoliang.wei@usst.edu.cn)

F. E. Alsaadi is with the Department of Electrical and Computer Engineering, Faculty of Engineering, King Abdulaziz University, Jeddah 21589, Saudi Arabia.

\* Corresponding author.

inequality method. So far, a large number of important results have appeared on the  $\ell_2$ - $\ell_\infty$  state estimation problems for various systems such as time-delay systems, complex networks, nonlinear systems, neural networks and sensor networks, see e.g. [12], [26], [27], [31], [38] and the references therein.

It is well recognized that, in classical control systems, the integral actions are able to eliminate the steady-state error of the controlled systems and enhance the insensitivity to parameter changes and system noises [1], [2], [28], [41], [42]. Similarly, by introducing an additional integral term of the output estimation error, the so-called proportional-integral observer (PIO) has been developed in order to achieve the desired accuracy and robustness [3]. In particular, the integral term in PIO can be regarded as an extension of the integral action in the traditional proportional-integral controller, which provides certain extra degree of freedom for the observer design. So far, the PIOs have been widely applied in reaching adequate tradeoff between the performance indices of robustness, disturbance rejection and loop recurrence for a range of complex dynamic systems [16], [32]. For instance, the PIO has been designed in [6] for a class of multiple-input-multiple-output linear systems in the interest of simultaneously estimating the system states and the unknown inputs, and the PIO design problem has been investigated in [39] for Takagi-Sugeno fuzzy system with hope to estimate the actuator and sensor faults.

As is well known, the phenomenon of time-delays appears frequently in practical engineering systems because of a variety of reasons such as equipment aging and transmission lags [20], [38]. Time-delays serve as one of the major sources for performance deterioration and system instability. Consequently, time-delay systems have been attracting an ever-increasing research interest and abundant theoretical/empirical literature has been available on examining the impact of time-delays on the dynamical behaviors of the underlying systems [14], [43]. According to the patterns they behave, the time-delays can be roughly categorized into discrete-time delays and distributed time-delays [29]. It should be mentioned that it is quite common for modern industrial systems to exhibit multiple types of time-delays (also known as mixed delays) due to the complexity and large scale of their structures. Accordingly, much research attention has recently been devoted to the analysis and synthesis problems for systems with mixed time-delays, see [18], [22], [25] for some representative work. Up to date, the PIO design problem in presence of mixed time-delays has not been fully investigated owing mainly to the lack of appropriate methodologies, and such a situation inspires our current investigation in order to bridge the gap.

Networked systems (NSs) are well known for their outstanding capability in sharing resources and improving system diagnosability as well as maintainability, and have therefore been successfully applied in key areas ranging from intelligent transportation, aerospace, industrial control, telemedicine to robotic teleoperation [4], [5], [10], [11]. In NSs, all the system components (e.g. sensors, actuators, controllers/filters) act as network nodes that are connected via shared communication networks, and the data is transmitted by using network-based communication technology [13], [15], [17], [21], [40], [45]. In engineering practice, the data collision is often unavoidable due mainly to the limited bandwidth and service capacity of the network, and the resulting network-induced phenomena have placed great challenges on the control/filtering problems of NSs. An effective way of avoiding/mitigating data collision is to deploy the communication protocols to regulate the transmission orders among the network nodes, and some typical communication protocols are Round-Robin protocol (RRP), Try-Once-Discard protocol and stochastic communication protocol [7], [19], [33], [44]. It should be noted that the adoption of communication protocols in NSs gives rise to essential difficulties in analyzing/synthesizing NSs, for

example, the establishment of an appropriate mathematical model to depict the scheduling mechanism of communication protocols and the development of a theoretical framework for revealing the impact of scheduling behavior on the control/filtering performance.

In recent years, the RRP (also known as the token ring protocol) has been utilized extensively in the fields of communication and signal processing [30], [43]. The RRP refers to a static scheduling protocol in which the nodes are assigned the access to transmission according to a preset circular order. To be more specific, under the scheduling of the RRP, the node that obtains the access token at current transmission instant will pass the “token” to the next node at next transmission instant. When the data transmission of the last node is completed, the access token will be handed over to the first node. Up to date, the state estimation problems under RRP have begun to stir some research interest and preliminary results have been available in the literature [9], [35]. For instance, the state estimation problem under RRP has been studied for complex networks [43], genetic regulatory networks [34], and neural networks [31]. In fact, most of the existing results on the RRP-based state estimation issues have focused on the design of Kalman filters or Luenberger observers. When it comes to the RRP-based PIO design problem, the corresponding results have been very few (if not none) due mainly to the increased complexity and computation burden caused by the “periodic” nature of the RRP. With this in mind, we aim to deal with the PIO design problem for a class of discrete-time systems with mixed time-delays under RRP.

Based on the above discussions, it can be summarized that: 1) the  $\ell_2\text{-}\ell_\infty$  state estimation approach serves as a powerful means in improving robustness of the system and restraining the effect from the energy-bounded disturbance input on the estimation error; and 2) the PIO design problem under RRP is of both practical importance and theoretical significance. In view of this, we endeavor to design an  $\ell_2\text{-}\ell_\infty$  PIO for systems with mixed time-delays under RRP, which is an emerging research topic that exhibits substantial difficulties in dealing with the complexity in embedding the RRP in the PIO design procedure as well as in analyzing the stability and  $\ell_2\text{-}\ell_\infty$  performance of the estimation error dynamics.

The main contributions of this paper are highlighted as follows: 1) *a PIO design problem is, for the first time, proposed for a class of systems with mixed time-delays under the RRP*; 2) *a token-dependent PIO is designed to cope with the effects of the RRP scheduling behavior on the estimation performance*; and 3) *a novel Lyapunov functional, which is dependent on the order of data transmission, is constructed to facilitate the analysis of the exponential stability and the  $\ell_2\text{-}\ell_\infty$  performance of the estimation error dynamics*. The remainder of this paper is arranged as follows. Section II formulates the PIO design problem for systems with mixed time-delays and presents the mathematical description of the RRP. In Section III, sufficient conditions are derived for the analysis of the exponential stability, the  $\ell_2\text{-}\ell_\infty$  performance of the systems as well as the existence of the desired PIO, respectively. Section IV provides a simulation example and Section V gives the conclusion of this paper.

**Notation.** The notation in this paper is standard except where otherwise stated.  $\mathbb{Z}^-$  denotes the set of all nonpositive integers and  $\mathbb{N}$  represents the set of all nonnegative integers, respectively. The symbol  $\delta(m, n)$  denotes the Kronecker delta function that equals 1 (when  $m = n$ ) and equals 0 (when  $m \neq n$ ), and the function  $\text{mod}(u, v)$  means the unique non-negative remainder on division of the integer  $u$  by the positive integer  $v$ . In particular, we denote  $\mathfrak{N} \triangleq \{1, 2, \dots, n\}$ .

## II. PROBLEM FORMULATION AND PRELIMINARIES

Consider the following discrete-time system with mixed time-delays:

$$\begin{cases} x(k+1) = Ax(k) + B \sum_{d=1}^{\infty} \varrho_d x(k-d) + Mv(k) \\ \quad + Dx(k - \varsigma(k)) \\ z(k) = Hx(k) \\ x(j) = \varphi(j), \quad \forall j \in \mathbb{Z}^- \end{cases} \quad (1)$$

where  $x(k) \in \mathbb{R}^{n_x}$  is the state vector,  $z(k) \in \mathbb{R}^{n_z}$  is the output vector to be estimated, and  $v(k) \in \mathbb{R}^{n_v}$  is the exogenous disturbance input belonging to  $\ell_2[0, +\infty)$ .  $\varphi(j)$  is a given initial condition sequence.  $A$ ,  $B$ ,  $D$ ,  $M$  and  $H$  are known real constant matrices with appropriate dimensions.

*Assumption 1:* The positive integer  $\varsigma(k)$  satisfies

$$\varsigma_m \leq \varsigma(k) \leq \varsigma_M, \quad k \in \mathbb{N}$$

where  $\varsigma_m$  and  $\varsigma_M$  are known positive integers.

*Assumption 2:* The constants  $\varrho_d \geq 0$  ( $d = 1, 2, \dots$ ) satisfy the following convergence condition:

$$\bar{\varrho} := \sum_{d=1}^{\infty} \varrho_d \leq \sum_{d=1}^{\infty} d\varrho_d < +\infty. \quad (2)$$

*Remark 1:* In the considered system (1), the positive integer  $\varsigma(k)$  represents the discrete time-varying delay and the term  $\sum_{d=1}^{\infty} \varrho_d x(k-d)$  describes the infinitely distributed delay in the form of discrete-time case. The convergence condition in Assumption 2 is provided to guarantee the convergence of both the term  $B \sum_{d=1}^{\infty} \varrho_d x(k-d)$  and the Lyapunov functional presented later.

### A. Communication Network

It is assumed that the system information is collected by  $n$  sensors and the corresponding measurement on sensor  $i$  is

$$y_i(k) = C_i x(k) + F_i w(k), \quad i \in \mathfrak{N} \quad (3)$$

where  $y_i(k) \in \mathbb{R}^{n_y}$  and  $w(k) \in \mathbb{R}^{n_w}$  belonging to  $\ell_2[0, +\infty)$  are the measurement output and the measurement noise, respectively.  $C_i$  and  $F_i$  ( $i \in \mathfrak{N}$ ) are known real constant matrices with appropriate dimensions.

For presentation clarity, we denote

$$\begin{aligned} y(k) &\triangleq \begin{bmatrix} y_1^T(k) & y_2^T(k) & \cdots & y_n^T(k) \end{bmatrix}^T \\ C &\triangleq \begin{bmatrix} C_1^T & C_2^T & \cdots & C_n^T \end{bmatrix}^T \\ F &\triangleq \begin{bmatrix} F_1^T & F_2^T & \cdots & F_n^T \end{bmatrix}^T. \end{aligned}$$

Then, the measurement outputs of system (1) can be rewritten as the following compact form:

$$y(k) = Cx(k) + Fw(k). \quad (4)$$

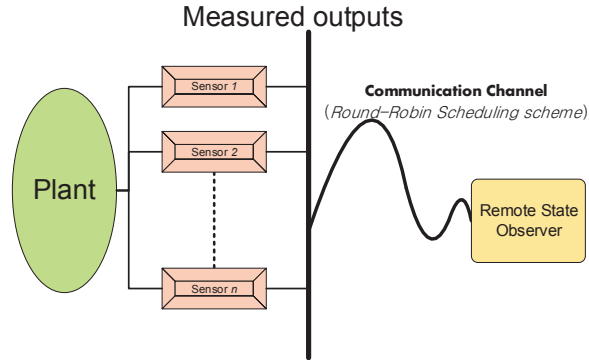


Fig. 1: State estimation under Round-Robin protocol.

As shown in Fig. 1, there are  $n$  sensors to transmit their measurements to the state observer via the communication network. However, due to the limited communication capacity of the network, data collision might occur in case of simultaneous transmissions of large amount of data which, in turn, leads to many adverse network-induced phenomena (e.g. fading measurements, data disorder and dropouts). In view of this, a periodical scheduling scheme, namely, the RRP, is adopted here to orchestrate the data transmissions.

Let  $\check{y}_i(k)$  denote the measurement of the  $i$ th sensor after transmission with a zero-order holder (ZOH) strategy. The updating of  $\check{y}_i(k)$  under RRP can be written as

$$\check{y}_i(k) = \begin{cases} y_i(k), & \text{if } i = \tau(k) \\ \check{y}_i(k-1), & \text{otherwise} \end{cases} \quad (5)$$

where  $\tau(k) \triangleq \text{mod}(k-1, n) + 1$  ( $\tau(k) \in \mathfrak{N}$ ) represents the selected sensor at time instant  $k$ .

Denoting  $\check{y}(k) = [\check{y}_1^T(k) \ \check{y}_2^T(k) \ \cdots \ \check{y}_n^T(k)]^T$ , we can further express the actually received measurement  $\check{y}(k)$  as

$$\check{y}(k) = \Psi_{\tau(k)} y(k) + (I - \Psi_{\tau(k)}) \check{y}(k-1) \quad (6)$$

where  $\Psi_i \triangleq \text{diag}\{\delta(i, 1), \delta(i, 2), \dots, \delta(i, n)\}$  and  $\delta(\cdot, \cdot) \in \{0, 1\}$  is the Kronecker delta function.

*Remark 2:* The so-called RRP has been widely deployed in industry owing to its distinct merits in improving the network utilization and reducing the communication burden [9], [30], [35]. Nevertheless, the RRP is also a potential factor contributing to the deterioration of system performance due to the orchestration of the data transmission order and the change of the update rule. According to the scheduling scheme of RRP, at each transmission instant, only one sensor gains access to the communication network and sends corresponding measurement data to the observer. In view of this, a ZOH strategy is adopted in this paper with hope to make the best utilization of the received measurements.

Letting  $\eta(k) \triangleq \begin{bmatrix} x^T(k) & \check{y}^T(k-1) \end{bmatrix}^T$  and  $\vartheta(k) \triangleq \begin{bmatrix} v^T(k) & w^T(k) \end{bmatrix}^T$ , the system (1) with the RRP can be reformulated as follows:

$$\left\{ \begin{array}{l} \eta(k+1) = \mathcal{A}_{\tau(k)}\eta(k) + \mathcal{B} \sum_{d=1}^{\infty} \varrho_d \eta(k-d) \\ \quad + \mathcal{D}\eta(k - \varsigma(k)) + \mathcal{M}_{\tau(k)}\vartheta(k) \\ \check{y}(k) = \mathcal{C}_{\tau(k)}\eta(k) + \mathcal{F}_{\tau(k)}\vartheta(k) \\ z(k) = \mathcal{H}\eta(k) \\ \eta(j) = \check{\varphi}(j), \quad \forall j \in \mathbb{Z}^- \end{array} \right. \quad (7)$$

where  $\check{\varphi}(j) \triangleq \begin{bmatrix} \varphi^T(j) & 0_{1 \times nn_y} \end{bmatrix}^T$  and

$$\begin{aligned} \mathcal{A}_{\tau(k)} &\triangleq \begin{bmatrix} A & 0_{n_x \times nn_y} \\ \Psi_{\tau(k)}C & I - \Psi_{\tau(k)} \end{bmatrix} \\ \mathcal{M}_{\tau(k)} &\triangleq \begin{bmatrix} M & 0_{n_x \times n_w} \\ 0_{nn_y \times n_v} & \Psi_{\tau(k)}F \end{bmatrix} \\ \mathcal{C}_{\tau(k)} &\triangleq \begin{bmatrix} \Psi_{\tau(k)}C & I - \Psi_{\tau(k)} \end{bmatrix} \\ \mathcal{F}_{\tau(k)} &\triangleq \begin{bmatrix} 0_{nn_y \times n_v} & \Psi_{\tau(k)}F \end{bmatrix} \\ \mathcal{B} &\triangleq \begin{bmatrix} B & 0_{n_x \times nn_y} \\ 0_{nn_y \times n_x} & 0_{nn_y \times nn_y} \end{bmatrix} \\ \mathcal{D} &\triangleq \begin{bmatrix} D & 0_{n_x \times nn_y} \\ 0_{nn_y \times n_x} & 0_{nn_y \times nn_y} \end{bmatrix} \\ \mathcal{H} &\triangleq \begin{bmatrix} H & 0_{n_z \times nn_y} \end{bmatrix}. \end{aligned}$$

### B. The proportional-integral observer

For the purpose of estimating the states of the system (7), we construct a token-dependent PIO of the following form:

$$\left\{ \begin{array}{l} \hat{\eta}(k+1) = \mathcal{A}_{\tau(k)}\hat{\eta}(k) + \mathcal{B} \sum_{d=1}^{\infty} \varrho_d \hat{\eta}(k-d) \\ \quad + \mathcal{D}\hat{\eta}(k - \varsigma(k)) + L_{\tau(k)}^I \zeta(k) \\ \quad + L_{\tau(k)}^P (\check{y}(k) - \mathcal{C}_{\tau(k)}\hat{\eta}(k)) \\ \zeta(k+1) = \zeta(k) + K_{\tau(k)} (\check{y}(k) - \mathcal{C}_{\tau(k)}\hat{\eta}(k)) \\ \hat{z}(k) = \mathcal{H}\hat{\eta}(k) \\ \hat{\eta}(j) = 0, \quad \forall j \in \mathbb{Z}^- \end{array} \right. \quad (8)$$

where  $\hat{\eta}(k) \in \mathbb{R}^{n_\eta}$  with  $n_\eta = n_x + nn_y$  is the estimate of  $\eta(k)$ ,  $\hat{z}(k) \in \mathbb{R}^{n_z}$  is the estimate of  $z(k)$ , and  $\zeta(k) \in \mathbb{R}^{n_\zeta}$  is a vector representing the integral of the weighted output estimation error.  $L_{\tau(k)}^P$ ,  $L_{\tau(k)}^I$  and  $K_{\tau(k)}$  are the observer gain matrices to be designed.

*Remark 3:* It should be emphasized that, different from the conventional Luenberger observer, PIO can *not only* utilize the current information in the proportional term *but also* exploit the historical information in the integral term. In addition, the PIO presented in (8), whose gains are related to the order of data transmission, is accomplished to cope with the impact from the protocol-induced periodic nature on the observer design. More specifically, the periodic scheduling behavior of the RRP is reflected in the observer structure by the token-dependent matrices  $L_{\tau(k)}^P$ ,  $L_{\tau(k)}^I$  and  $K_{\tau(k)}$ , which can be obtained by solving a set of linear matrix inequalities (LMIs) relating to the periodic scheduling signal  $\tau(k)$ .

Letting  $\tilde{\eta}(k) \triangleq \eta(k) - \hat{\eta}(k)$  and  $\tilde{z}(k) \triangleq z(k) - \hat{z}(k)$ , we obtain the estimation error dynamics from (7) and (8) as follows:

$$\left\{ \begin{array}{l} \tilde{\eta}(k+1) = (\mathcal{A}_{\tau(k)} - L_{\tau(k)}^P \mathcal{C}_{\tau(k)}) \tilde{\eta}(k) - L_{\tau(k)}^I \zeta(k) \\ \quad + \mathcal{B} \sum_{d=1}^{\infty} \varrho_d \tilde{\eta}(k-d) + \mathcal{D} \tilde{\eta}(k - \varsigma(k)) \\ \quad + (\mathcal{M}_{\tau(k)} - L_{\tau(k)}^P \mathcal{F}_{\tau(k)}) \vartheta(k) \\ \tilde{z}(k) = \mathcal{H} \tilde{\eta}(k) \\ \tilde{\eta}(j) = \check{\varphi}(j), \quad \forall j \in \mathbb{Z}^- \end{array} \right. \quad (9)$$

Then, by setting  $\xi(k) \triangleq [\tilde{\eta}^T(k) \quad \zeta^T(k)]^T$ , we have the following augmented system:

$$\left\{ \begin{array}{l} \xi(k+1) = \mathcal{A}_{\tau(k)} \xi(k) + \mathcal{B} \sum_{d=1}^{\infty} \varrho_d \xi(k-d) \\ \quad + \mathcal{D} \xi(k - \varsigma(k)) + \mathcal{M}_{\tau(k)} \vartheta(k) \\ \tilde{z}(k) = \mathcal{H} \xi(k) \\ \xi(j) = \psi(j), \quad \forall j \in \mathbb{Z}^- \end{array} \right. \quad (10)$$

where

$$\begin{aligned} \mathcal{A}_{\tau(k)} &\triangleq \begin{bmatrix} \mathcal{A}_{\tau(k)} - L_{\tau(k)}^P \mathcal{C}_{\tau(k)} & -L_{\tau(k)}^I \\ K_{\tau(k)} \mathcal{C}_{\tau(k)} & I \end{bmatrix} \\ \mathcal{M}_{\tau(k)} &\triangleq \begin{bmatrix} \mathcal{M}_{\tau(k)} - L_{\tau(k)}^P \mathcal{F}_{\tau(k)} \\ K_{\tau(k)} \mathcal{F}_{\tau(k)} \end{bmatrix} \\ \mathcal{B} &\triangleq \begin{bmatrix} \mathcal{B} & 0_{n_{\eta} \times n_{\zeta}} \\ 0_{n_{\zeta} \times n_{\eta}} & 0_{n_{\zeta} \times n_{\zeta}} \end{bmatrix}, \quad \psi(j) \triangleq \begin{bmatrix} \check{\varphi}(j) \\ 0_{n_{\zeta} \times 1} \end{bmatrix} \\ \mathcal{D} &\triangleq \begin{bmatrix} \mathcal{D} & 0_{n_{\eta} \times n_{\zeta}} \\ 0_{n_{\zeta} \times n_{\eta}} & 0_{n_{\zeta} \times n_{\zeta}} \end{bmatrix}, \quad \mathcal{H} \triangleq \begin{bmatrix} \mathcal{H} & 0_{n_z \times n_{\zeta}} \end{bmatrix}. \end{aligned}$$

For facilitating the subsequent analysis, the definition of exponential stability is given as follows.

*Definition 1:* The augmented system (10) with  $\vartheta(k) = 0$  is said to be exponentially stable if there exist constants  $\iota > 0$  and  $\epsilon \in (0, 1)$  such that

$$\|\xi(k)\|^2 \leq \iota \epsilon^k \sup_{j \in \mathbb{Z}^-} \|\psi(j)\|^2, \quad \forall k \in \mathbb{N}. \quad (11)$$

The aim of this paper is to design a  $\ell_2$ - $\ell_{\infty}$  PIO for discrete-time system with mixed time-delays and RRP scheduling effects such that the following requirements are satisfied simultaneously:

- 1) the augmented system (10) with  $\vartheta(k) = 0$  is exponentially stable;
- 2) for a given scalar  $\gamma > 0$  representing disturbance attenuation level and all non-zero  $\vartheta(k)$ , under the zero-initial condition, the augmented system (10) satisfies the following  $\ell_2$ - $\ell_\infty$  performance constraint:

$$\sup_k \sqrt{\tilde{z}^T(k)\tilde{z}(k)} < \gamma \sqrt{\sum_{k=0}^{\infty} \|\vartheta(k)\|^2}. \quad (12)$$

### III. MAIN RESULTS

In this section, we first analyze the exponential stability for the augmented system (10). Then, a sufficient condition is established to meet the  $\ell_2$ - $\ell_\infty$  performance constraint (12). Finally, the desired PIO gain matrices are obtained by solving the token-dependent LMIs.

The following lemma is useful for further technical development.

*Lemma 1:* [29] Let  $\chi_l \in \mathbb{R}^{n_\xi}$  with  $n_\xi = n_\eta + n_\zeta$ , scalar constants  $m_l \geq 0$  ( $l = 1, 2, \dots$ ) and  $Z \in \mathbb{R}^{n_\xi \times n_\xi}$  be a positive semi-definite matrix. The following inequality always holds:

$$\left( \sum_{l=1}^{\infty} m_l \chi_l \right)^T Z \left( \sum_{l=1}^{\infty} m_l \chi_l \right) \leq \left( \sum_{l=1}^{\infty} m_l \right) \sum_{l=1}^{\infty} m_l \chi_l^T Z \chi_l.$$

#### A. Exponential Stability Analysis

In this subsection, a sufficient condition on the exponential stability of the augmented system (10) is presented by constructing the token-dependent Lyapunov functional.

*Theorem 1:* Let the PIO gain matrices  $L_i^P$ ,  $L_i^I$  and  $K_i$  ( $i \in \mathfrak{N}$ ) be given. The augmented system (10) is exponentially stable with  $\vartheta(k) = 0$  if there exist positive-definite matrices  $P_i$ ,  $Q$  and  $R$  such that

$$\Xi_i = \begin{bmatrix} \Xi_i^{11} & * \\ \Xi_i^{21} & \Xi_i^{22} \end{bmatrix} < 0 \quad (13)$$

where

$$\begin{aligned} \Xi_i^{11} &\triangleq \text{diag}\{\mathcal{P}_i, -Q, -\frac{1}{\bar{\rho}}R\} \\ \Xi_i^{21} &\triangleq \begin{bmatrix} \mathcal{A}_i & \mathcal{B} & \mathcal{D} \end{bmatrix} \\ \Xi_i^{22} &\triangleq -P_{i+1}^{-1} \\ \mathcal{P}_i &\triangleq -P_i + \bar{\rho}R + (\varsigma_M - \varsigma_m + 1)Q \end{aligned}$$

with  $P_{n+1} = P_1$  for all  $i \in \mathfrak{N}$ .

*Proof:* In order to examine the exponential stability of the augmented system (10), we choose the following token-dependent Lyapunov functional candidate:

$$V_{\tau(k)}(k) = V_{1,\tau(k)}(k) + \sum_{j=2}^4 V_j(k) \quad (14)$$

where

$$V_{1,\tau(k)}(k) \triangleq \xi^T(k) P_{\tau(k)} \xi(k)$$



$$\begin{aligned}
V_2(k) &\triangleq \sum_{s=k-\varsigma(k)}^{k-1} \xi^T(s)Q\xi(s) \\
V_3(k) &\triangleq \sum_{t=k-\varsigma_M+1}^{k-\varsigma_m} \sum_{s=t}^{k-1} \xi^T(s)Q\xi(s) \\
V_4(k) &\triangleq \sum_{d=1}^{\infty} \varrho_d \sum_{r=k-d}^{k-1} \xi^T(r)R\xi(r).
\end{aligned}$$

Along the trajectory of the system (10) with  $\vartheta(k) = 0$ , the difference of  $V_{1,\tau(k)}(k)$  is calculated as follows:

$$\begin{aligned}
&\Delta V_{1,\tau(k)}(k) \\
&= V_{1,\tau(k+1)}(k+1) - V_{1,\tau(k)}(k) \\
&= \xi^T(k+1)P_{\tau(k+1)}\xi(k+1) - \xi^T(k)P_{\tau(k)}\xi(k) \\
&= \left( \mathcal{A}_{\tau(k)}\xi(k) + \mathcal{B} \sum_{d=1}^{\infty} \varrho_d \xi(k-d) + \mathcal{D}\xi(k-\varsigma(k)) \right)^T \\
&\quad \times P_{\tau(k+1)} \left( \mathcal{A}_{\tau(k)}\xi(k) + \mathcal{B} \sum_{d=1}^{\infty} \varrho_d \xi(k-d) + \mathcal{D} \right. \\
&\quad \left. \times \xi(k-\varsigma(k)) \right) - \xi^T(k)P_{\tau(k)}\xi(k) \\
&= \xi^T(k) \left( \mathcal{A}_{\tau(k)}^T P_{\tau(k+1)} \mathcal{A}_{\tau(k)} - P_{\tau(k)} \right) \xi(k) + 2\xi^T(k) \\
&\quad \times \mathcal{A}_{\tau(k)}^T P_{\tau(k+1)} \mathcal{B} \left( \sum_{d=1}^{\infty} \varrho_d \xi(k-d) \right) + 2\xi^T(k) \mathcal{A}_{\tau(k)}^T \\
&\quad \times P_{\tau(k+1)} \mathcal{D} \xi(k-\varsigma(k)) + \left( \sum_{d=1}^{\infty} \varrho_d \xi(k-d) \right)^T \mathcal{B}^T \\
&\quad \times P_{\tau(k+1)} \mathcal{B} \left( \sum_{d=1}^{\infty} \varrho_d \xi(k-d) \right) + 2 \left( \sum_{d=1}^{\infty} \varrho_d \xi(k-d) \right)^T \\
&\quad \times \mathcal{B}^T P_{\tau(k+1)} \mathcal{D} \xi(k-\varsigma(k)) + \xi^T(k-\varsigma(k)) \mathcal{D}^T P_{\tau(k+1)} \\
&\quad \times \mathcal{D} \xi(k-\varsigma(k)). \tag{15}
\end{aligned}$$

Furthermore, we also have

$$\begin{aligned}
&\Delta V_2(k) \\
&= V_2(k+1) - V_2(k) \\
&= \sum_{s=k-\varsigma(k+1)+1}^k \xi^T(s)Q\xi(s) - \sum_{s=k-\varsigma(k)}^{k-1} \xi^T(s)Q\xi(s) \\
&= \xi^T(k)Q\xi(k) - \xi^T(k-\varsigma(k))Q\xi(k-\varsigma(k)) \\
&\quad + \sum_{s=k-\varsigma(k+1)+1}^{k-1} \xi^T(s)Q\xi(s) - \sum_{s=k-\varsigma(k)+1}^{k-1} \xi^T(s)Q\xi(s)
\end{aligned}$$

$$\begin{aligned}
&= \xi^T(k)Q\xi(k) - \xi^T(k - \varsigma(k))Q\xi(k - \varsigma(k)) \\
&\quad + \sum_{s=k-\varsigma_M+1}^{k-1} \xi^T(s)Q\xi(s) + \sum_{s=k-\varsigma(k+1)+1}^{k-\varsigma_M} \xi^T(s)Q\xi(s) \\
&\quad - \sum_{s=k-\varsigma(k)+1}^{k-1} \xi^T(s)Q\xi(s) \\
&\leq \xi^T(k)Q\xi(k) - \xi^T(k - \varsigma(k))Q\xi(k - \varsigma(k)) \\
&\quad + \sum_{s=k-\varsigma_M+1}^{k-\varsigma_M} \xi^T(s)Q\xi(s) \tag{16} \\
&\Delta V_3(k) \\
&= V_3(k+1) - V_3(k) \\
&= \sum_{t=k-\varsigma_M+2}^{k-\varsigma_M+1} \sum_{s=t}^k \xi^T(s)Q\xi(s) - \sum_{t=k-\varsigma_M+1}^{k-\varsigma_M} \sum_{s=t}^k \xi^T(s)Q\xi(s) \\
&= \sum_{t=k-\varsigma_M+1}^{k-\varsigma_M} \left( \xi^T(k)Q\xi(k) - \xi^T(t)Q\xi(t) \right) \\
&= (\varsigma_M - \varsigma_M)\xi^T(k)Q\xi(k) - \sum_{s=k-\varsigma_M+1}^{k-\varsigma_M} \xi^T(s)Q\xi(s). \tag{17}
\end{aligned}$$

In addition, based on Lemma 1, it is obtained that

$$\begin{aligned}
&\Delta V_4(k) \\
&= V_4(k+1) - V_4(k) \\
&= \sum_{d=1}^{\infty} \varrho_d \sum_{r=k-d+1}^k \xi^T(r)R\xi(r) - \sum_{d=1}^{\infty} \varrho_d \sum_{r=k-d}^{k-1} \xi^T(r)R\xi(r) \\
&= \bar{\varrho}\xi^T(k)R\xi(k) - \sum_{d=1}^{\infty} \varrho_d \xi^T(k-d)R\xi(k-d) \\
&\leq \bar{\varrho}\xi^T(k)R\xi(k) - \frac{1}{\bar{\varrho}} \left( \sum_{d=1}^{\infty} \varrho_d \xi(k-d) \right)^T R \left( \sum_{d=1}^{\infty} \varrho_d \xi(k-d) \right). \tag{18}
\end{aligned}$$

By taking (15)-(18) into account, one has

$$\begin{aligned}
&\Delta V_{\tau(k)}(k) \\
&= \Delta V_{1,\tau(k)}(k) + \Delta V_2(k) + \Delta V_3(k) + \Delta V_4(k) \\
&\leq \xi^T(k) \left( \mathcal{A}_{\tau(k)}^T P_{\tau(k+1)} \mathcal{A}_{\tau(k)} + (\varsigma_M - \varsigma_M + 1)Q + \bar{\varrho}R \right. \\
&\quad \left. - P_{\tau(k)} \right) \xi(k) + \xi^T(k - \varsigma(k)) \left( \mathcal{D}^T P_{\tau(k+1)} \mathcal{D} - Q \right) \\
&\quad \times \xi(k - \varsigma(k)) + \left( \sum_{d=1}^{\infty} \varrho_d \xi(k-d) \right)^T \left( \mathcal{B}^T P_{\tau(k+1)} \right.
\end{aligned}$$

$$\begin{aligned}
& \times \mathcal{B} - \frac{1}{\bar{\varrho}} R \left( \sum_{d=1}^{\infty} \varrho_d \xi(k-d) \right) + 2\xi^T(k - \varsigma(k)) \mathcal{D}^T \\
& \times P_{\tau(k+1)} \mathcal{A}_{\tau(k)} \xi(k) + 2 \left( \sum_{d=1}^{\infty} \varrho_d \xi(k-d) \right)^T \mathcal{B}^T \\
& \times P_{\tau(k+1)} \mathcal{A}_{\tau(k)} \xi(k) + 2 \left( \sum_{d=1}^{\infty} \varrho_d \xi(k-d) \right)^T \mathcal{B}^T \\
& \times P_{\tau(k+1)} \mathcal{D} \xi(k - \varsigma(k)).
\end{aligned} \tag{19}$$

For notational convenience, we denote

$$\aleph_1(k) \triangleq \begin{bmatrix} \xi(k) \\ \xi(k - \varsigma(k)) \\ \sum_{d=1}^{\infty} \varrho_d \xi(k-d) \end{bmatrix}.$$

Accordingly, it is readily inferred that

$$\Delta V_{\tau(k)}(k) \leq \aleph_1^T(k) \Pi_{\tau(k)} \aleph_1(k). \tag{20}$$

where

$$\begin{aligned}
\Pi_{\tau(k)} & \triangleq \begin{bmatrix} \Pi_{\tau(k)}^{11} & * & * \\ \Pi_{\tau(k)}^{21} & \Pi_{\tau(k)}^{22} & * \\ \Pi_{\tau(k)}^{31} & \Pi_{\tau(k)}^{32} & \Pi_{\tau(k)}^{33} \end{bmatrix} \\
\Pi_{\tau(k)}^{11} & \triangleq -P_{\tau(k)} + \mathcal{A}_{\tau(k)}^T P_{\tau(k+1)} \mathcal{A}_{\tau(k)} \\
& \quad + \bar{\varrho} R + (\varsigma_M - \varsigma_m + 1) Q \\
\Pi_{\tau(k)}^{21} & \triangleq \mathcal{D}^T P_{\tau(k+1)} \mathcal{A}_{\tau(k)} \\
\Pi_{\tau(k)}^{22} & \triangleq -Q + \mathcal{D}^T P_{\tau(k+1)} \mathcal{D} \\
\Pi_{\tau(k)}^{31} & \triangleq \mathcal{B}^T P_{\tau(k+1)} \mathcal{A}_{\tau(k)} \\
\Pi_{\tau(k)}^{32} & \triangleq \mathcal{B}^T P_{\tau(k+1)} \mathcal{D} \\
\Pi_{\tau(k)}^{33} & \triangleq -\frac{1}{\bar{\varrho}} R + \mathcal{B}^T P_{\tau(k+1)} \mathcal{B}.
\end{aligned}$$

In the light of Schur Complement Lemma, we conclude from (13) that  $\Pi_{\tau(k)} < 0$ , which further indicates

$$\Delta V_{\tau(k)}(k) \leq -\lambda_{\min}(-\Pi_{\tau(k)}) \|\xi(k)\|^2. \tag{21}$$

In what follows, we shall proceed to analyze the exponential stability of the augmented system (10). According to the definition of  $V_{\tau(k)}(k)$  and (2), we know that

$$V_{\tau(k)}(k) \leq \eta_1 \|\xi(k)\|^2 + \eta_2 \sum_{t=k-\varsigma_M}^{k-1} \|\xi(t)\|^2 + \eta_3 \sup_{j \in \mathbb{Z}^-} \|\psi(j)\|^2 \tag{22}$$

where

$$\begin{aligned}
\eta_1 & \triangleq \lambda_{\max}(P_{\tau(k)}), \quad \eta_2 \triangleq (\bar{h} - \underline{h} + 1) \lambda_{\max}(Q) \\
\eta_3 & \triangleq \varrho \lambda_{\max}(R), \quad \varrho \triangleq \sum_{d=1}^{\infty} d \varrho_d.
\end{aligned}$$

Furthermore, for any  $\rho > 1$ , it follows from (21) that

$$\begin{aligned}
& \rho^{k+1}V_{\tau(k+1)}(k+1) - \rho^kV_{\tau(k)}(k) \\
&= \rho^{k+1}\Delta V_{\tau(k)}(k) + \rho^{k+1}V_{\tau(k)}(k) - \rho^kV_{\tau(k)}(k) \\
&\leq \rho^{k+1}\left(-\lambda_{\min}(-\Pi_{\tau(k)})\|\xi(k)\|^2\right) + \rho^k(\rho-1)V_{\tau(k)}(k) \\
&\leq \alpha_1(\rho)\rho^k\|\xi(k)\|^2 + \eta_3 \sup_{j \in \mathbb{Z}^-} \|\psi(j)\|^2 + \alpha_2(\rho) \sum_{t=k-\varsigma_M}^{k-1} \rho^k\|\xi(t)\|^2.
\end{aligned} \tag{23}$$

where

$$\begin{aligned}
\alpha_1(\rho) &\triangleq -\lambda_{\min}(-\Pi_{\tau(k)})\rho + (\rho-1)\eta_1 \\
\alpha_2(\rho) &\triangleq (\rho-1)\eta_2.
\end{aligned}$$

For any integer  $\theta \geq 1$ , taking summation on both sides of (23) from 0 to  $\theta-1$  with respect to  $k$  yields

$$\begin{aligned}
& \rho^\theta V_{\tau(\theta)}(\theta) - V_{\tau(0)}(0) \\
&\leq \alpha_1(\rho) \sum_{k=0}^{\theta-1} \rho^k \|\xi(k)\|^2 + \eta_3 \sup_{j \in \mathbb{Z}^-} \|\psi(j)\|^2 \\
&\quad + \alpha_2(\rho) \sum_{k=0}^{\theta-1} \sum_{t=k-\varsigma_M}^{k-1} \rho^k \|\xi(t)\|^2.
\end{aligned} \tag{24}$$

Additionally, the last item in (24) can be computed as

$$\begin{aligned}
& \sum_{k=0}^{\theta-1} \sum_{t=k-\varsigma_M}^{k-1} \rho^k \|\xi(t)\|^2 \\
&\leq \left( \sum_{t=-\varsigma_M}^{-1} \sum_{k=0}^{t+\varsigma_M} + \sum_{t=0}^{\theta-\varsigma_M-1} \sum_{k=t+1}^{t+\varsigma_M} + \sum_{t=\theta-\varsigma_M}^{\theta-1} \sum_{k=t+1}^{\theta-1} \right) \rho^k \|\xi(t)\|^2 \\
&\leq \frac{\rho^{\varsigma_M} - 1}{\rho - 1} \sum_{t=-\varsigma_M}^{-1} \|\xi(t)\|^2 + \frac{\rho(\rho^{\varsigma_M} - 1)}{\rho - 1} \sum_{t=0}^{\theta-1} \rho^t \|\xi(t)\|^2 \\
&\quad + \frac{\rho(\rho^{\varsigma_M} - 1)}{\rho - 1} \sum_{t=0}^{\theta-1} \rho^t \|\xi(t)\|^2.
\end{aligned} \tag{25}$$

Then, it follows from (24) and (25) that

$$\begin{aligned}
& \rho^\theta V_{\tau(\theta)}(\theta) - V_{\tau(0)}(0) \\
&\leq \alpha_1(\rho) \sum_{k=0}^{\theta-1} \rho^k \|\xi(k)\|^2 + \eta_3 \sup_{j \in \mathbb{Z}^-} \|\psi(j)\|^2 + \alpha_2(\rho) \left( \frac{\rho^{\varsigma_M} - 1}{\rho - 1} \sum_{t=-\varsigma_M}^{-1} \|\xi(t)\|^2 \right. \\
&\quad \left. + \frac{\rho(\rho^{\varsigma_M} - 1)}{\rho - 1} \sum_{t=0}^{\theta-1} \rho^t \|\xi(t)\|^2 + \frac{\rho(\rho^{\varsigma_M} - 1)}{\rho - 1} \sum_{t=0}^{\theta-1} \rho^t \|\xi(t)\|^2 \right) \\
&\leq \beta_1(\rho) \sum_{k=0}^{\theta-1} \rho^k \|\xi(k)\|^2 + \beta_2(\rho) \sup_{j \in \mathbb{Z}^-} \|\psi(j)\|^2
\end{aligned} \tag{26}$$

where

$$\begin{aligned}\beta_1(\rho) &\triangleq \alpha_1(\rho) + \alpha_2(\rho) \frac{2\rho^{\varsigma_M+1} - 2\rho}{\rho - 1} \\ \beta_2(\rho) &\triangleq \alpha_2(\rho) \varsigma_M \frac{\rho^{\varsigma_M} - 1}{\rho - 1} + \eta_3.\end{aligned}$$

Since  $\beta_1(1) = -\lambda_{\min}(-\Pi_{\tau(k)}) < 0$  and  $\lim_{\rho \rightarrow \infty} \beta_1(\rho) = +\infty$ , we can infer that there exists a scalar  $\gamma > 1$  such that  $\beta_1(\gamma) = 0$ , which implies that

$$\gamma^\theta V_{\tau(\theta)}(\theta) - V_{\tau(0)}(0) \leq \beta_2(\gamma) \sup_{j \in \mathbb{Z}^-} \|\psi(j)\|^2. \quad (27)$$

Noting

$$V_{\tau(0)}(0) \leq \bar{\eta} \sup_{j \in \mathbb{Z}^-} \|\psi(j)\|^2 \quad (28)$$

with

$$\bar{\eta} \triangleq (\varsigma_M + 2) \max\{\eta_1, \eta_2, \eta_3\},$$

and

$$\gamma^\theta V_{\tau(\theta)}(\theta) \geq \lambda_{\min}(P_{\tau(\theta)}) \gamma^\theta \|\xi(\theta)\|^2, \quad (29)$$

we obtain

$$\begin{aligned}\|\xi(\theta)\|^2 &\leq \frac{\bar{\eta} + \beta_2(\gamma)}{\lambda_{\min}(P_{\tau(\theta)}) \gamma^\theta} \sup_{j \in \mathbb{Z}^-} \|\psi(j)\|^2 \\ &= \lambda \pi^\theta \sup_{j \in \mathbb{Z}^-} \|\psi(j)\|^2\end{aligned} \quad (30)$$

with

$$\lambda \triangleq \frac{\bar{\eta} + \beta_2(\gamma)}{\lambda_{\min}(P_{\tau(\theta)})}, \quad \pi \triangleq \frac{1}{\gamma}.$$

Consequently, according to Definition 1, it is easy to conclude that the augmented system (10) is exponentially stable, which completes the proof.  $\blacksquare$

### B. $\ell_2$ - $\ell_\infty$ Performance Analysis

In this subsection, we shall give a sufficient condition to analyze the  $\ell_2$ - $\ell_\infty$  performance of the system (10) under the zero initial condition.

*Theorem 2:* Let the PIO gain matrices  $L_i^P, L_i^I, K_i$  ( $i \in \mathfrak{N}$ ) and the disturbance attenuation level  $\gamma > 0$  be given. The system (10) is exponentially stable and satisfies the  $\ell_2$ - $\ell_\infty$  performance constraint (12) for all non-zero  $\vartheta(k)$  under the zero-initial condition if there exist positive-definite matrices  $P_i, Q$  and  $R$  such that

$$\left\{ \begin{aligned} \Theta_i &= \begin{bmatrix} \Theta_i^{11} & * \\ \Theta_i^{21} & \Xi_i^{22} \end{bmatrix} < 0 \\ \Phi_i &= \begin{bmatrix} -P_i & * \\ \mathcal{H} & -I \end{bmatrix} < 0 \end{aligned} \right. \quad (31a)$$

$$(31b)$$

where

$$\Theta_i^{11} \triangleq \text{diag}\{\mathcal{P}_i, -Q, -\frac{1}{\bar{\rho}}R, -\gamma^2 I\}$$

$$\Theta_i^{21} \triangleq \begin{bmatrix} \mathcal{A}_i & \mathcal{B} & \mathcal{D} & \mathcal{M}_i \end{bmatrix}$$

with  $P_{n+1} = P_1$  for all  $i \in \mathfrak{N}$ .

*Proof:* It is obvious that  $\Theta_i < 0$  implies  $\Xi_i < 0$ , hence it follows from Theorem 1 that the augmented system (10) is exponentially stable.

Next, let us analyze the  $\ell_2$ - $\ell_\infty$  performance of the augmented system (10) with any non-zero  $\vartheta(k)$ . For this purpose, define the following index functional:

$$\mathcal{J}(k) = V_{\tau(k)}(k) - \gamma^2 \sum_{s=0}^{k-1} \vartheta(s)^T \vartheta(s). \quad (32)$$

Under the initial condition  $\xi(0) = 0$ , we can easily have  $V(0) = 0$ , which results in

$$\begin{aligned} \mathcal{J}(k) &= V_{\tau(k)}(k) - \gamma^2 \sum_{s=0}^{k-1} \vartheta^T(s) \vartheta(s) \\ &= \sum_{s=0}^{k-1} \left( \Delta V_{\tau(s)}(s) - \gamma^2 \vartheta^T(s) \vartheta(s) \right) + V(0) \\ &\leq \sum_{s=0}^{k-1} \left( \aleph_1^T(s) \Pi_{\tau(s)} \aleph_1(s) + 2\xi^T(s) \mathcal{A}_{\tau(s)}^T P_{\tau(s+1)} \right. \\ &\quad \times \mathcal{M}_{\tau(s)} \vartheta(s) + 2 \left( \sum_{d=1}^{\infty} \varrho_d \xi(s-d) \right)^T \mathcal{B}^T \\ &\quad \times P_{\tau(s+1)} \mathcal{M}_{\tau(s)} \vartheta(s) + 2\xi^T(k - \varsigma(s)) \mathcal{D}^T \\ &\quad \times P_{\tau(s+1)} \mathcal{M}_{\tau(s)} \vartheta(s) + \vartheta^T(s) \mathcal{M}_{\tau(s)}^T P_{\tau(s+1)} \\ &\quad \left. \times \mathcal{M}_{\tau(s)} \vartheta(s) - \gamma^2 \vartheta^T(s) \vartheta(s) \right) \\ &= \sum_{s=0}^{k-1} \aleph_2^T(s) \Upsilon_{\tau(s)} \aleph_2(s) \end{aligned} \quad (33)$$

where

$$\aleph_2(k) \triangleq \begin{bmatrix} \xi(k) \\ \xi(k - \varsigma(k)) \\ \sum_{d=1}^{\infty} \varrho_d \xi(k-d) \\ \vartheta(k) \end{bmatrix}$$

$$\Upsilon_{\tau(k)} \triangleq \begin{bmatrix} \Pi_{\tau(k)}^{11} & * & * & * \\ \Pi_{\tau(k)}^{21} & \Pi_{\tau(k)}^{22} & * & * \\ \Pi_{\tau(k)}^{31} & \Pi_{\tau(k)}^{32} & \Pi_{\tau(k)}^{33} & * \\ \Upsilon_{\tau(k)}^{41} & \Upsilon_{\tau(k)}^{42} & \Upsilon_{\tau(k)}^{43} & \Upsilon_{\tau(k)}^{44} \end{bmatrix}$$

$$\Upsilon_{\tau(k)}^{41} \triangleq \mathcal{M}_{\tau(k)}^T P_{\tau(k+1)} \mathcal{A}_{\tau(k)}$$

$$\Upsilon_{\tau(k)}^{42} \triangleq \mathcal{M}_{\tau(k)}^T P_{\tau(k+1)} \mathcal{D}$$

$$\begin{aligned}\Upsilon_{\tau(k)}^{43} &\triangleq \mathcal{M}_{\tau(k)}^T P_{\tau(k+1)} \mathcal{B} \\ \Upsilon_{\tau(k)}^{44} &\triangleq \mathcal{M}_{\tau(k)}^T P_{\tau(k+1)} \mathcal{M}_{\tau(k)} - \gamma^2 I.\end{aligned}$$

By virtue of Schur Complement Lemma, it is concluded from (31a) that  $\mathcal{J}(k) < 0$ , which further indicates that

$$\begin{aligned}\xi^T(k) P_{\tau(k)} \xi(k) &= V_{1,\tau(k)}(k) \\ &< V_{\tau(k)}(k) < \gamma^2 \sum_{s=0}^{k-1} \vartheta^T(s) \vartheta(s).\end{aligned}\quad (34)$$

Furthermore, (31b) implies

$$\tilde{z}^T(k) \tilde{z}(k) = \xi^T(k) \mathcal{H}^T \mathcal{H} \xi(k) < \xi^T(k) P_{\tau(k)} \xi(k). \quad (35)$$

Combining with (34), it is easy to see that

$$\tilde{z}^T(k) \tilde{z}(k) < \gamma^2 \sum_{s=0}^{k-1} \vartheta^T(s) \vartheta(s). \quad (36)$$

Taking both the supremum of  $\tilde{z}^T(k) \tilde{z}(k)$  over  $k$  and the limit of  $\sum_{s=0}^{k-1} \vartheta^T(s) \vartheta(s)$  with  $k \rightarrow \infty$ , we obtain

$$\sup_k \tilde{z}^T(k) \tilde{z}(k) < \gamma^2 \sum_{s=0}^{\infty} \vartheta^T(s) \vartheta(s) \quad (37)$$

and thus

$$\sup_k \sqrt{\tilde{z}^T(k) \tilde{z}(k)} < \gamma \sqrt{\sum_{k=0}^{\infty} \|\vartheta(k)\|^2} \quad (38)$$

for all non-zero  $\vartheta(k)$ , which completes the proof.  $\blacksquare$

### C. PIO Design

In this subsection, a sufficient condition is given for the existence of the desired PIO that is capable of ensuring both the exponential stability and the  $\ell_2$ - $\ell_\infty$  performance.

*Theorem 3:* Let the disturbance attenuation level  $\gamma > 0$  be given. The system (10) is exponentially stable and satisfies the  $\ell_2$ - $\ell_\infty$  performance constraint (12) for all non-zero  $\vartheta(k)$  under the zero-initial condition if there exist positive-definite matrices  $\acute{P}_i, \grave{P}_i$  ( $i \in \mathfrak{N}$ ),  $\acute{Q}, \grave{Q}, \acute{R}, \grave{R}$  and matrices  $\acute{L}_i^P, \acute{L}_i^I, \grave{K}_i$  ( $i \in \mathfrak{N}$ ) such that

$$\begin{cases} \acute{\Theta}_i = \begin{bmatrix} \acute{\Theta}_i^{11} & * \\ \acute{\Theta}_i^{21} & \acute{\Theta}_i^{22} \end{bmatrix} < 0 \end{cases} \quad (39a)$$

$$\begin{cases} \acute{\Phi}_i = \begin{bmatrix} -P_i & * \\ \mathcal{H} & -I \end{bmatrix} < 0 \end{cases} \quad (39b)$$

where

$$\acute{\Theta}_i^{11} \triangleq \text{diag}\{\acute{\mathcal{P}}_i, -Q, -\frac{1}{\bar{\rho}}R, -\gamma^2 I\}$$

$$\begin{aligned}
\Theta_i^{21} &\triangleq [\mathcal{A}_i \ \mathcal{B}_i \ \mathcal{D}_i \ \mathcal{M}_i] \\
\Theta_i^{22} &\triangleq \text{diag}\{-\dot{P}_{i+1}, -\dot{P}_{i+1}\} \\
\mathcal{A}_i &\triangleq \begin{bmatrix} \dot{P}_{i+1}\mathcal{A}_i - \dot{L}_i^P\mathcal{C}_i & -\dot{L}_i^I \\ \dot{K}_i\mathcal{C}_i & \dot{P}_{i+1} \end{bmatrix} \\
\mathcal{M}_i &\triangleq \begin{bmatrix} \dot{P}_{i+1}\mathcal{M}_i - \dot{L}_i^P\mathcal{F}_i \\ \dot{K}_i\mathcal{F}_i \end{bmatrix} \\
\mathcal{B}_i &\triangleq \begin{bmatrix} \dot{P}_{i+1}\mathcal{B} & 0_{n_\eta \times n_\zeta} \\ 0_{n_\zeta \times n_\eta} & 0_{n_\zeta \times n_\zeta} \end{bmatrix} \\
\mathcal{D}_i &\triangleq \begin{bmatrix} \dot{P}_{i+1}\mathcal{D} & 0_{n_\eta \times n_\zeta} \\ 0_{n_\zeta \times n_\eta} & 0_{n_\zeta \times n_\zeta} \end{bmatrix} \\
P_i &\triangleq \text{diag}\{\dot{P}_i, \dot{P}_i\}, \quad Q \triangleq \text{diag}\{\dot{Q}, \dot{Q}\} \\
R &\triangleq \text{diag}\{\dot{R}, \dot{R}\}, \quad \tilde{P}_i \triangleq \text{diag}\{\dot{P}_i, \dot{P}_i\} \\
\dot{P}_i &\triangleq -\dot{P}_i + \bar{\rho}\dot{R} + (\varsigma_M - \varsigma_m + 1)\dot{Q} \\
\dot{P}_i &\triangleq -\dot{P}_i + \bar{\rho}\dot{R} + (\varsigma_M - \varsigma_m + 1)\dot{Q}
\end{aligned}$$

with  $\dot{P}_{n+1} = \dot{P}_1$  and  $\dot{P}_{n+1} = \dot{P}_1$  for all  $i \in \mathfrak{N}$ . In addition, the desired PIO gains are determined by

$$\begin{aligned}
L_i^P &= \dot{P}_{i+1}^{-1} \dot{L}_i^P \\
L_i^I &= \dot{P}_{i+1}^{-1} \dot{L}_i^I \\
K_i &= \dot{P}_{i+1}^{-1} \dot{K}_i, \quad (i \in \mathfrak{N}).
\end{aligned} \tag{40}$$

*Proof:* Performing the congruence transformation to the inequality (31a) by  $\text{diag}\{I, I, I, I, \dot{P}_{i+1}, \dot{P}_{i+1}\}$ , we have

$$\dot{\Theta}_i = \begin{bmatrix} \Theta_i^{11} & * \\ \Theta_i^{21} & \Theta_i^{22} \end{bmatrix} < 0 \tag{41}$$

where

$$\dot{\Theta}_i^{21} \triangleq \begin{bmatrix} \dot{P}_{i+1}\mathcal{A}_i - \dot{P}_{i+1}L_i^P\mathcal{C}_i & -\dot{P}_{i+1}L_i^I & \dot{P}_{i+1}\mathcal{B} \\ \dot{P}_{i+1}K_i\mathcal{C}_i & \dot{P}_{i+1} & 0 \\ 0 & \dot{P}_{i+1}\mathcal{D} & 0 & \mathcal{M}_i - \dot{P}_{i+1}L_i^P\mathcal{F}_i \\ 0 & 0 & 0 & \dot{P}_{i+1}K_i\mathcal{F}_i \end{bmatrix}.$$

Utilizing the variable substitution

$$\begin{aligned}
\dot{L}_i^P &= \dot{P}_{i+1}L_i^P \\
\dot{L}_i^I &= \dot{P}_{i+1}L_i^I \\
\dot{K}_i &= \dot{P}_{i+1}K_i, \quad (i \in \mathfrak{N})
\end{aligned} \tag{42}$$

we conclude that (41) is ensured by (39a). Thereafter, it is verified that the desired PIO gains are obtained by (40), which completes the proof.  $\blacksquare$



*Remark 4:* In this paper, a  $\ell_2$ - $\ell_\infty$  PIO has been first proposed to handle the state estimation issue for a class of mixed time-delay systems under RRP. By constructing a token-dependent Lyapunov functional, sufficient conditions have been derived in Theorems 1-2 to guarantee the exponential stability and  $\ell_2$ - $\ell_\infty$  performance of the estimation error system. In addition, the gains of the desired PIO has been obtained in Theorem 3 by solving a set of token-dependent LMIs.

*Remark 5:* Note that, the PIO design scheme provided is in form of LMI techniques. As is well known, the algorithm based on the standard LMI system has a polynomial-time complexity. That is, the number  $\mathcal{S}(\varepsilon)$  of flops needed to compute an  $\varepsilon$ -accurate solution is bounded by  $O(\mathcal{S}\mathcal{T}^3 \log(\mathcal{V}/\varepsilon))$ , where  $\mathcal{S}$  is the total row size of the LMI system,  $\mathcal{T}$  is the total number of scalar decision variables,  $\mathcal{V}$  is a data-dependent scaling factor, and  $\varepsilon$  is the relative accuracy set for algorithm [43]. For the investigated discrete-time system (1) with the RRP (5), the variable dimensions can be seen from  $x(k) \in \mathbb{R}^{n_x}$ ,  $y(k) \in \mathbb{R}^{n_y}$ ,  $z(k) \in \mathbb{R}^{n_z}$  and  $\zeta(k) \in \mathbb{R}^{n_\zeta}$ . From Theorem 3, we have  $\mathcal{S} = 4n_x + 4nn_y + 4n_\zeta + n_z$  and  $\mathcal{T} = 2n_x^2 + 4n_y n_x + 3(nn_y)^2 + (nn_\zeta + n)nn_y + 3n_\zeta^2 + (n_x + n_y)n_\zeta + 1$ . Therefore, the computational complexity of the LMIs-based PIO design algorithm with regard to the RRP can be represented as  $O(n_x^7 + n_y^7 + n_\zeta^7)$ , which depends polynomially on the number of sensors and the variable dimensions.

*Remark 6:* Our main results are distinguished from some existing ones by the following features: 1) the problem investigated in this paper is novel in the sense that the PIO is, for the first time, designed for a class of mixed time-delay systems under RRP; and 2) the token-dependent PIO is novel, which reflects the protocol-induced periodic nature in the observer structure, and thus reduces the conservatism in the design procedure.

#### IV. NUMERICAL SIMULATION

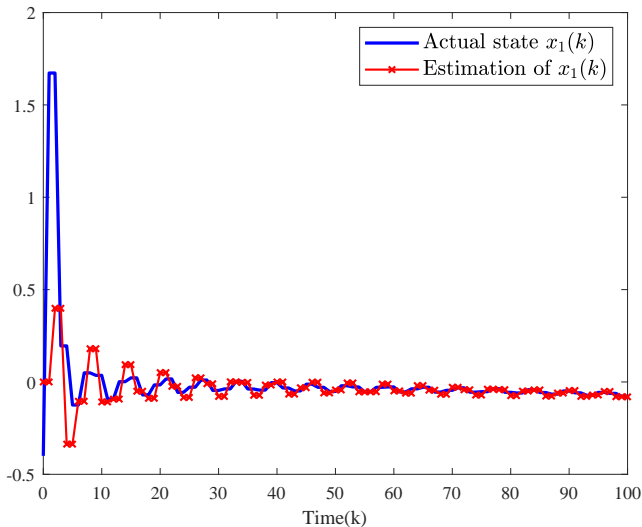


Fig. 2: Trajectories of state  $x_1(k)$  and its estimation.

In this section, we shall propose a simulation example for the sake of illustrating the validity and superiority of the designed PIO.

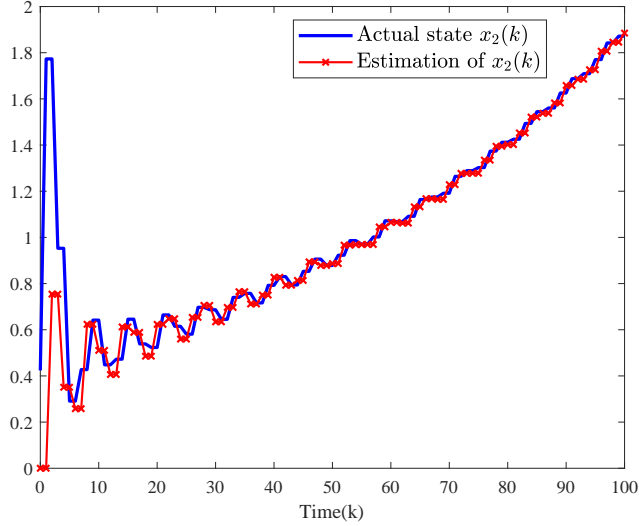


Fig. 3: Trajectories of state  $x_2(k)$  and its estimation.

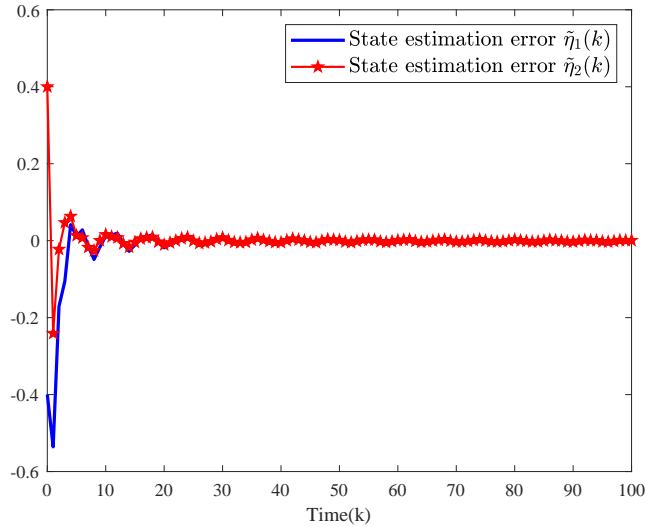


Fig. 4: Trajectories of the state estimation error  $\tilde{\eta}(k)$  with PIO.

Consider a target system given by (1) with corresponding parameters chosen as follows:

$$A = \begin{bmatrix} 0.59 & 0.42 \\ 0.31 & 0.34 \end{bmatrix}, \quad B = \begin{bmatrix} 0.42 & 0.53 \\ 0.04 & 0.21 \end{bmatrix}$$

$$D = \begin{bmatrix} 0.18 & 0.11 \\ -0.02 & 0.1 \end{bmatrix}, \quad M = \begin{bmatrix} 0.12 \\ -0.08 \end{bmatrix}, \quad H = \begin{bmatrix} 1.41 \\ 2.82 \end{bmatrix}^T.$$

In addition, we assume that  $n = 2$  and the output measurements are modeled by the following parameters:

$$C_1 = \begin{bmatrix} 0.97 & 4.1 \end{bmatrix}, \quad F_1 = 0.25$$

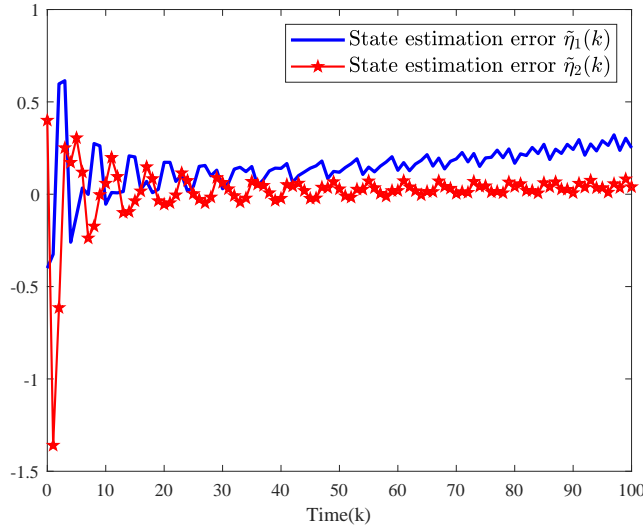


Fig. 5: Trajectories of the state estimation error  $\tilde{\eta}(k)$  with Luenberger observer.

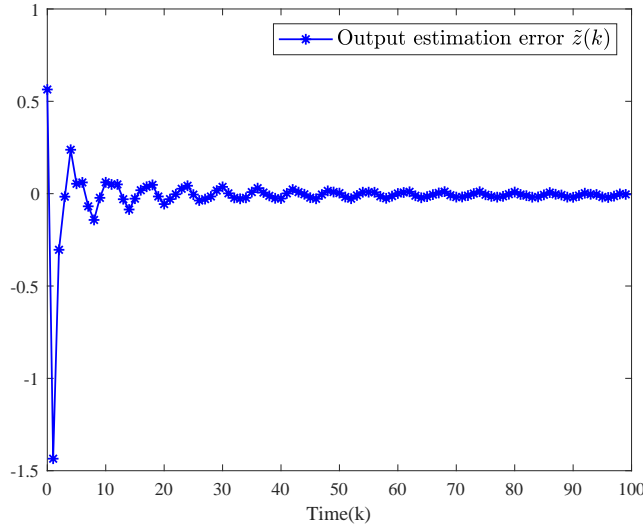


Fig. 6: Trajectory of the output estimation error  $\tilde{z}(k)$ .

$$C_2 = \begin{bmatrix} 2.49 & 1.41 \end{bmatrix}, \quad F_2 = 0.41.$$

In the simulation, the external disturbance and the measurement noise are set to be  $v(k) = 0.5e^{-0.2k} \cos(k)$  and  $w(k) = \frac{4 \sin(k)}{k+1}$ , respectively. The initial conditions are taken as  $x(j) = \begin{bmatrix} -0.4 & 0.4 \end{bmatrix}^T$  ( $j \in \mathbb{Z}^-$ ). The constant  $\varrho_d = 2^{-(d+3)}$ , it can be easily verified that  $\bar{\varrho} = \sum_{d=1}^{\infty} \varrho_d = 2^{-4} < \sum_{d=1}^{\infty} d\varrho_d = (2^4 \ln 2)^{-1} < \infty$ , which means that the convergence condition (2) is met. The time-varying delay is chosen as  $\varsigma(k) = 2 + \cos(k\pi)$ , from which we can easily check that  $\varsigma_m \leq \varsigma(k) \leq \varsigma_M$  with  $\varsigma_m = 1$  and  $\varsigma_M = 3$ .

With the aid of MATLAB software (with the YALMIP 3.0), the solutions to LMIs (39a) and (39b) can

be obtained immediately as follows:

$$\begin{aligned} \dot{P}_1 &= \begin{bmatrix} 3.2962 & 0.2347 & 0.5623 & 0.2718 \\ 0.2347 & 9.2982 & 1.5477 & 0.9262 \\ 0.5623 & 1.5477 & 6.3123 & 1.5146 \\ 0.2718 & 0.9262 & 1.5146 & 3.6667 \end{bmatrix}, \dot{P}_1 = 8.1585 \\ \dot{P}_2 &= \begin{bmatrix} 1.8418 & 1.2401 & 0.2896 & 0.3634 \\ 1.2401 & 8.0955 & 0.7533 & 0.8671 \\ 0.2896 & 0.7533 & 5.1256 & 1.8656 \\ 0.3634 & 0.8671 & 1.8656 & 5.8449 \end{bmatrix}, \dot{P}_2 = 2.9232 \\ \dot{Q} &= \begin{bmatrix} 0.7263 & 1.0394 & 0.0607 & 0.0511 \\ 1.0394 & 2.4875 & 0.2151 & 0.2238 \\ 0.0607 & 0.2151 & 1.5083 & 0.4884 \\ 0.0511 & 0.2238 & 0.4884 & 1.1913 \end{bmatrix}, \dot{Q} = 0.5950 \\ \dot{R} &= \begin{bmatrix} 0.4197 & 0.1376 & 0.0095 & 0.0099 \\ 0.1376 & 0.6690 & 0.0032 & 0.0044 \\ 0.0095 & 0.0032 & 0.4370 & 0.0020 \\ 0.0099 & 0.0044 & 0.0020 & 0.4349 \end{bmatrix}, \dot{R} = 0.4298. \end{aligned}$$

By virtue of the above solutions, the desired PIO gains can be calculated as follows:

$$\begin{aligned} L_1^P &= \begin{bmatrix} 0.2226 & -0.0043 \\ 0.1388 & -0.0021 \\ 0.9986 & 2.7676 \\ -0.0002 & 1.0001 \end{bmatrix}, L_1^I = \begin{bmatrix} -0.0047 \\ -0.0025 \\ -0.0141 \\ -0.0011 \end{bmatrix} \\ L_2^P &= \begin{bmatrix} -0.0057 & 0.2450 \\ -0.0058 & 0.1421 \\ 1.0002 & 1.9382 \\ -0.0037 & 0.9988 \end{bmatrix}, L_2^I = \begin{bmatrix} -0.0042 \\ -1.4034 \\ -4.7197 \\ -0.0085 \end{bmatrix} \\ K_1 &= \begin{bmatrix} 0.05962 & 0.2539 \end{bmatrix}, K_2 = \begin{bmatrix} 0.1562 & 0.0118 \end{bmatrix}. \end{aligned}$$

TABLE I: Minimal disturbance attenuation level for utilizing Luenberger observer and PIO

	PIO	Luenberger observer
$\bar{\gamma}$	1.0638	1.3534

Note that the disturbance attenuation level  $\gamma$  is predetermined in Theorems 2-3. In fact,  $\gamma$  can be optimized by replacing  $\gamma^2$  with  $\hat{\gamma}$  in Theorems 2-3, provided that it is not predetermined. Denote the optimized  $\gamma$  as  $\bar{\gamma}$ . Then, the minimal disturbance attenuation level for utilizing Luenberger observer and PIO are provided in Table I. It can be concluded from Table I that a smaller disturbance attenuation

level can be achieved by utilizing PIO, which implies that PIO has stronger robustness than Luenberger observer.

In order to showcase the advantage of PIO, we design a Luenberger observer for the same system and the gains of Luenberger observer are calculated as follows:

$$L_1 = \begin{bmatrix} 0.2825 & 1.5060 \\ 0.1694 & 1.6548 \\ 1.0023 & 2.1018 \\ -5.8446 & 1.0009 \end{bmatrix}, \quad L_2 = \begin{bmatrix} -4.0438 & 0.2406 \\ -4.1599 & 0.1414 \\ 1.0043 & 4.7097 \\ 2.0904 & 1.0036 \end{bmatrix}.$$

For the sake of further verifying our theoretical results, the numerical simulation results are presented in Figs. 2-6. The state trajectories and their estimates are depicted in Figs. 2-3. Fig. 4 and Fig. 5 plot the state estimation error with PIO and Luenberger observer, respectively. It is easy to observe that the PIO proposed in this paper outperforms Luenberger observer adopted in most literature for estimation performance. Moreover, the output estimation error is described in Fig. 6. From the above simulation results, we can confirm that the desired PIO performs extremely well.

## V. CONCLUSION

In this paper, we have dealt with the  $\ell_2$ - $\ell_\infty$  PIO design problem for a kind of linear discrete-time systems with mixed time-delays and RRP scheduling effects. The RRP has been employed to orchestrate the signal transmission in the measurement channel (sensor-to-observer) with hope to prevent data transmission conflicts available and allocate communication resources reasonably. A novel PIO has been developed whose gains depend on the data transmission order regulated by the RRP. By constructing a token-dependent Lyapunov functional, sufficient conditions have been established for analyzing the exponential stability and  $\ell_2$ - $\ell_\infty$  performance of the estimation error dynamics. The desired PIO gains have been obtained in terms of the solutions to LMIs. In the end, the validity of the proposed PIO design approach has been illustrated via a simulation example. Future research topics would be the extension of the main results in this paper to 1) more complicated NSs under different communication protocols [9], [30], [33]; 2) the investigation on how the number of integrators in PIO affects the estimation performance and 3) the improvement of the state estimation performance by using some latest optimization algorithms [23], [24].

## REFERENCES

- [1] K. H. Ang, G. Chong and Y. Li, PID control system analysis, design, and technology, *IEEE Transactions on Control Systems Technology*, vol. 3, no. 4, pp. 559–576, Jul. 2005.
- [2] K. J. Åström, T. Hägglund, C. C. Hang and W. K. Ho, Automatic tuning and adaptation for PID controllers—a survey, *Control Engineering Practice*, vol. 1, no. 4, pp. 699–714, Aug. 1993.
- [3] S. Beale and B. Shafai, Robust control system design with a proportional integral observer, *International Journal of Control*, vol. 50, no. 1, pp. 97–111, Apr. 1989.
- [4] R. Caballero-Águila, A. Hermoso-Carazo and J. Linares-Pérez, Distributed fusion filters from uncertain measured outputs in sensor networks with random packet losses, *Information Fusion*, vol. 34, pp. 70–79, Mar. 2017.
- [5] A. Cetinkaya, H. Ishii and T. Hayakawa, Networked control under random and malicious packet losses, *IEEE Transactions on Automatic Control*, vol. 62, no. 5, pp. 2434–2449, May 2017.
- [6] J.-L. Chang, Applying discrete-time proportional integral observers for state and disturbance estimations, *IEEE Transactions on Automatic Control*, vol. 51, no. 5, pp. 814–818, May 2006.

- [7] Y. Chen, Z. Wang, L. Wang and W. Sheng, Finite-horizon  $H_\infty$  state estimation for stochastic coupled networks with random inner couplings using Round-Robin protocol, *IEEE Transactions on Cybernetics*, in press, DOI: 10.1109/TCYB.2020.3004288.
- [8] Y. Chen and W. X. Zheng,  $L_2$ - $L_\infty$  filtering for stochastic Markovian jump delay systems with nonlinear perturbations, *Signal Processing*, vol. 109, pp. 154–164, Apr. 2015.
- [9] D. Ding, Z. Wang, Q.-L. Han and G. Wei, Neural-network-based output-feedback control under round-robin scheduling protocols, *IEEE Transactions on Cybernetics*, vol. 49, no. 6, pp. 2372–2384, Jun. 2019.
- [10] D. Ding, Z. Wang and Q.-L. Han, A scalable algorithm for event-triggered state estimation with unknown parameters and switching topologies over sensor networks, *IEEE Transactions on Cybernetics*, in press, DOI:10.1109/TCYB.2019.2917543.
- [11] D. Ding, Z. Wang and Q.-L. Han, Neural-network-based output-feedback control with stochastic communication protocols, *Automatica*, vol. 106, pp. 221–229, Aug. 2019.
- [12] K. M. Grigoriadis and J. T. Watson, Reduced order  $H_\infty$  and  $\ell_2$ - $\ell_\infty$  filtering via linear matrix inequalities, *IEEE Transactions on Aerospace and Electronic Systems*, vol. 33, no. 4, pp. 1326–1338, Oct. 1997.
- [13] F. Han, G. Wei, D. Ding and Y. Song, Finite-horizon bounded  $H_\infty$  synchronisation and state estimation for discrete-time complex networks: Local performance analysis, *IET Control Theory & Applications*, vol. 11, no. 6, pp. 827–837, Apr. 2017.
- [14] J. Hu, Z. Wang, G.-P. Liu, H. Zhang and R. Navaratne, A prediction-based approach to distributed filtering with missing measurements and communication delays through sensor networks, *IEEE Transactions on Systems, Man, and Cybernetics-Systems*, in press, DOI: 10.1109/TSMC.2020.2966977.
- [15] J. Hu, Z. Wang, G.-P. Liu and H. Zhang, Variance-constrained recursive state estimation for time-varying complex networks with quantized measurements and uncertain inner coupling, *IEEE Transactions on Neural Networks and Learning Systems*, vol. 31, no. 6, pp. 1955–1967, Jun. 2020.
- [16] D. Koenig, Unknown input proportional multiple-integral observer design for linear descriptor systems: Application to state and fault estimation, *IEEE Transactions on Automatic Control*, vol. 50, no. 2, pp. 212–217, Feb. 2005.
- [17] W. Li, G. Wei, F. Han and Y. Liu, Weighted average consensus-based unscented Kalman filtering, *IEEE Transactions on Cybernetics*, vol. 46, no. 2, pp. 558–567, Feb. 2016.
- [18] H. Liu, Z. Wang, B. Shen and H. Dong, Delay-distribution-dependent  $H_\infty$  state estimation for discrete-time memristive neural networks with mixed time-delays and fading measurements, *IEEE Transactions on Cybernetics*, vol. 50, no. 2, pp. 440–451, Feb. 2020.
- [19] S. Liu, Z. Wang, Y. Chen and G. Wei, Protocol-based unscented Kalman filtering in the presence of stochastic uncertainties, *IEEE Transactions on Automatic Control*, vol. 65, no. 3, pp. 1303–1309, Mar. 2020.
- [20] Y. Liu, B. Shen and H. Shu, Finite-time resilient  $H_\infty$  state estimation for discrete-time delayed neural networks under dynamic event-triggered mechanism, *Neural Networks*, vol. 121, pp. 356–365, Jan. 2020.
- [21] Y. Liu, B. Shen and Q. Li, State estimation for neural networks with Markov-based nonuniform sampling: The partly unknown transition probability case, *Neurocomputing*, vol. 357, pp. 261–270, Sept. 2019.
- [22] Y. Liu, Z. Wang, L. Ma, Y. Cui and F. E. Alsaadi, Synchronization of directed switched complex networks with stochastic link perturbations and mixed time-delays, *Nonlinear Analysis: Hybrid Systems*, vol. 27, pp. 213–224, Feb. 2018.
- [23] Y. Liu, Q. Cheng, Y. Gan, Y. Wang, Z. Li and J. Zhao, Multi-objective optimization of energy consumption in crude oil pipeline transportation system operation based on exergy loss analysis, *Neurocomputing*, vol. 332, pp. 100–110, Mar. 2019.
- [24] Y. Liu, S. Chen, B. Guan and P. Xu, Layout optimization of large-scale oil-gas gathering system based on combined optimization strategy, *Neurocomputing*, vol. 332, pp. 159–183, Mar. 2019.
- [25] L. Ma, Z. Wang, Q.-L. Han and Y. Liu, Dissipative control for nonlinear Markovian jump systems with actuator failures and mixed time-delays, *Automatica*, vol. 98, pp. 358–362, Dec. 2018.
- [26] W. Qian, Y. Li, Y. Chen, and W. Liu,  $L_2$ - $L_\infty$  filtering for stochastic delayed systems with randomly occurring nonlinearities and sensor saturation, *International Journal of Systems Science*, in press, DOI: 10.1080/00207721.2020.1794080.
- [27] W. Qian, Y. Li, Y. Zhao, and Y. Chen, New optimal method for  $L_2$ - $L_\infty$  state estimation of delayed neural networks, *Neurocomputing*, vol. 415, pp. 258–265, 2020.
- [28] D. Rosinová and V. Veselý, Robust PID decentralized controller design using LMI, *International Journal of Computers Communications & Control*, vol. 2, no. 2, pp. 195–204, 2007.
- [29] B. Shen, Z. Wang and H. Tan, Guaranteed cost control for uncertain nonlinear systems with mixed time-delays: The discrete-time case, *European Journal of Control*, vol. 40, pp. 62–67, Mar. 2018.
- [30] B. Shen, Z. Wang, D. Wang and H. Liu, Distributed state-saturated recursive filtering over sensor networks under Round-Robin protocol, *IEEE Transactions on Cybernetics*, vol. 50, no. 8, pp. 3605–3615, Aug. 2020.
- [31] Y. Shen, Z. Wang, B. Shen, F. E. Alsaadi and A. M. Dobaie,  $\ell_2$ - $\ell_\infty$  state estimation for delayed artificial neural networks under high-rate communication channels with Round-Robin protocol, *Neural Networks*, vol. 124, pp. 170–179, Apr. 2020.
- [32] D. Söffker, T. J. Yu and P. C. Müller, State estimation of dynamical systems with nonlinearities by using proportional-integral observer, *International Journal of Systems Science*, vol. 26, no. 9, pp. 1571–1582, Nov. 1995.

- [33] X. Wan, Z. Wang, Q.-L. Han and M. Wu, Finite-time  $H_\infty$  state estimation for discrete time-delayed genetic regulatory networks under stochastic communication protocols, *IEEE Transactions on Circuits and Systems-Part I*, vol. 65, no. 10, pp. 3481–3491, Apr. 2018.
- [34] X. Wan, Z. Wang, M. Wu and X. Liu, State estimation for discrete time-delayed genetic regulatory networks with stochastic noises under the round-robin protocols, *IEEE Transactions on Nanobioscience*, vol. 17, no. 2, pp. 145–154, Apr. 2018.
- [35] F. Wang, Z. Wang, J. Liang and X. Liu, Resilient filtering for linear time-varying repetitive processes under uniform quantizations and Round-Robin protocols, *IEEE Transactions on Circuits and Systems I: Regular Papers*, vol. 65, no. 9, pp. 2992–3004, Sept. 2018.
- [36] D. A. Wilson, Convolution and Hankel operator norms for linear systems, *IEEE Transactions on Automatic Control*, vol. 34, no. 1, pp. 94–97, Jan. 1989.
- [37] L. Wu and W. X. Zheng,  $L_2$ - $L_\infty$  control of nonlinear fuzzy Itô stochastic delay systems via dynamic output feedback, *IEEE Transactions on Systems, Man, and Cybernetics, Part B (Cybernetics)*, vol. 39, no. 5, pp. 1308–1315, Mar. 2009.
- [38] R. Yang, H. Gao and P. Shi, Delay-dependent  $L_2$ - $L_\infty$  filter design for stochastic time-delay systems, *IET Control Theory & Applications*, vol. 5, no. 1, pp. 1–8, Sept.–Oct. 2011.
- [39] T. Youssef, M. Chadli, H. R. Karimi and R. Wang, Actuator and sensor faults estimation based on proportional integral observer for TS fuzzy model, *Journal of the Franklin Institute*, vol. 354, no. 6, pp. 2524–2542, Apr. 2017.
- [40] X.-M. Zhang, Q.-L. Han and X. Yu, Survey on recent advances in networked control systems, *IEEE Transactions on Industrial Informatics*, vol. 12, no. 5, pp. 1740–1752, Oct. 2016.
- [41] D. Zhao, Z. Wang, G. Wei and Q.-L. Han, A dynamic event-triggered approach to observer-based PID security control subject to deception attacks, *Automatica*, vol. 120, Art. no. 109128, Oct. 2020.
- [42] D. Zhao, Z. Wang, D. W. C. Ho and G. Wei, Observer-based PID security control for discrete time-delay systems under cyber-attacks, *IEEE Transactions on Systems, Man, and Cybernetics-Systems*, in press, DOI: 10.1109/TSMC.2019.2952539.
- [43] L. Zou, Z. Wang, H. Gao and X. Liu, State estimation for discrete-time dynamical networks with time-varying delays and stochastic disturbances under the Round-Robin protocol, *IEEE Transactions on Neural Networks and Learning Systems*, vol. 28, no. 5, pp. 1139–1151, Feb. 2017.
- [44] L. Zou, Z. Wang, Q.-L. Han and D. Zhou, Moving horizon estimation for networked time-delay systems under Round-Robin protocol, *IEEE Transactions on Automatic Control*, vol. 64, no. 12, pp. 5191–5198, Dec. 2019.
- [45] L. Zou, Z. Wang and D. H. Zhou, Moving horizon estimation with non-uniform sampling under component-based dynamic event-triggered transmission, *Automatica*, vol. 120, Art. no. 109154, Oct. 2020.